☙

Low-energy coherent Stoner-like excitations in CaFe₂As₂

Liqin Ke,[1,2] Mark van Schilfgaarde,[1] Jiji Pulikkotil,[2] Takao Kotani,[3] and Vladimir Antropov[2]

[1]*School of Materials, Arizona State University, Tempe, AZ 85287*
[2]*Ames Laboratory USDOE, Ames, IA 50011*
[3]*Tottori University, Tottori, 680-8552, Japan*

Using linear-response density functional theory, magnetic excitations in the striped phase of CaFe₂As₂ are studied as a function of local-moment amplitude. We find a new kind of excitation: sharp resonances of Stoner-like (itinerant) excitations at energies comparable to the Néel temperature, originating largely from a narrow band of Fe d states near the Fermi level, and coexisting with more conventional (localized) spin waves. Both kinds of excitations can show multiple branches, highlighting the inadequacy of a description based on a localized spin model.

Magnetic interactions are likely to play a key role in mediating superconductivity in the recently discovered family of iron pnictides; however, their character is not yet well understood.[1–3] In particular, whether the system is best described in terms of large, local magnetic moments centered at each Fe site, in which case elementary excitations are collective spin waves (SWs) or are itinerant (elementary excitations characterized by single-particle electron-hole transitions) is a subject of great debate. This classification also depends on the energy scale of interest. The most relevant energy scale in CaFe₂As₂ and other pnictides ranges to about twice the Néel temperature, i.e., $2T_N \approx 40$ meV. Unfortunately, neutron scattering experiments have focused on the character of excitations in the 150–200 meV range,[4,5] much larger than energy that stabilizes observed magnetism or superconductivity. Experiments in Refs. 4 and 5, while very similar, take completely different points of view concerning the magnetic excitations that they observe. There is a similar dichotomy in theoretical analyses of magnetic interactions.[6,7] Model descriptions usually postulate a local-moments picture.[8] Most *ab initio* studies start from the local spin-density approximation (LSDA) to density functional theory. While the LSDA traditionally favors itinerant magnetism (weak on-site Coulomb correlations), practitioners strongly disagree about the character of pnictides; indeed, the same results are used as proof of both localized and itinerant descriptions.[6,7]

The dynamic magnetic susceptibility (DMS) is the central quantity that uniquely characterizes magnetic excitations. It can elucidate the origins of magnetic interactions and distinguish between localized and itinerant character. However, it is difficult to compute in practice; studies to date have been limited to a few simple systems. Here, we adapt an all-electron linear-response technique developed recently[9,10] to calculate the transverse DMS $\chi(\mathbf{q},\omega)$. Aside from SWs seen in neutron scattering, we find low-energy particle-hole excitations at low q and also at high q. In stark contrast to conventional particle-hole excitations in the Stoner continuum, they can be sharply peaked in energy (resonances) and can be measured.

The full transverse DMS $\chi(\mathbf{r},\mathbf{r}',\mathbf{q},\omega)$ is a function of coordinates $\mathbf{r}$ and $\mathbf{r}'$ (confined to the unit cell). It is obtained from the noninteracting susceptibility $\chi_0(\mathbf{r},\mathbf{r}',\mathbf{q},\omega)$ via the standard relation[11]

$$\chi = \chi_0(1 - \chi_0 I)^{-1}, \tag{1}$$

where I is the exchange-correlation kernel. When computed within the time-dependent LSDA, I is local: $I = I(\mathbf{r})\delta(\mathbf{r} - \mathbf{r}')$.[11] The χ_0 can be obtained from the band structure using the all-electron methodology that we developed.[9,10] The Imχ_0 originates from spin-flip transitions between occupied states at $\mathbf{k}$ and unoccupied states at $\mathbf{k} + \mathbf{q}$: it is a k-resolved joint density of states D decorated by products P of four wave functions[10]

$$D(\mathbf{k},\mathbf{q},\omega) = f(\epsilon_\mathbf{k}^\uparrow)[1 - f(\epsilon_{\mathbf{q}+\mathbf{k}}^\downarrow)]\delta(\omega - \epsilon_{\mathbf{q}+\mathbf{k}}^\downarrow + \epsilon_\mathbf{k}^\uparrow), \tag{2}$$

$$\mathrm{Im}\chi_0^{+-} = \int d\omega\, d^3\mathbf{k}\, P(\mathbf{r},\mathbf{r}',\mathbf{k},\mathbf{q}) \times D(\mathbf{k},\mathbf{q},\omega). \tag{3}$$

Because of the computational burden that Eq. (3) poses, we make a simplification, mapping χ_0 onto the local magnetization density, which is assumed to rotate rigidly. The full $\chi_0(\mathbf{r},\mathbf{r}',\mathbf{q},\omega)$ simplifies to the discrete matrix $\chi_0(\mathbf{R},\mathbf{R}',\mathbf{q},\omega)$ associated with pairs of magnetic sites $(\mathbf{R},\mathbf{R}')$ in the unit cell; $I(\mathbf{r})$ simplifies to a diagonal matrix $I_{\mathbf{RR}}$. In Ref. 10, we show that we need not compute I explicitly but can determine it from a sum rule. I can be identified with the Stoner parameter in models. We essentially follow the procedure described in detail in Ref. 10, and obtain $\chi(\mathbf{q},\omega)$ as a 4×4 matrix corresponding to the four Fe sites in the unit cell. For Fe and Ni, these approximations yield results in rather good agreement with the full time dependent LSDA results. To make a connection with neutron experiments, spectra are obtained from the matrix element $\sum_{\mathbf{R},\mathbf{R}'}\langle e^{i\mathbf{q}\cdot\mathbf{R}}|\chi(\mathbf{R},\mathbf{R}',\mathbf{q},\omega)|e^{i\mathbf{q}\cdot\mathbf{R}'}\rangle$. For brevity, we omit indices $\mathbf{RR}'$ henceforth.

We analyze the low-temperature (striped) phase of CaFe₂As₂ within the LSDA, and show how these states depend critically on the Zeeman field generated by the Fe magnetic moment M. We do this by varying the Fe–As bond length $R_{\mathrm{Fe-As}}$: its main effect is to control the magnetic moment M, which in turn strongly affects the character of magnetic interaction. Similar changes can be accomplished by other means (e.g., with the external B field), as we will report elsewhere. Results for tetragonal and orthorhombic striped
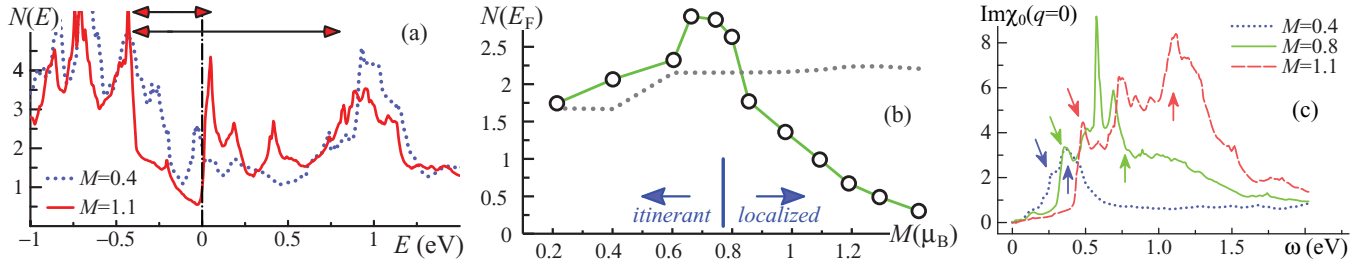
FIG. 1. (Color online) (a) $N(E)$ is shown in units of eV^{-1} per cell containing one Fe atom. Data are shown for $M = 0.4\mu_B$ and $1.1\mu_B$. Both kinds of transitions are reflected in peaks in $\chi_0(q = 0, \omega)$, shown in panel (c) for $M = 0.4\mu_B$, $0.8\mu_B$, and $1.1\mu_B$. (b) $N(E_F)$ is shown as a function of moment M. The blue vertical bar denotes the experimental moment. It also approximately demarcates the transition from itinerant to localized behavior. (c) The bare susceptibility $\chi_0(q = 0, \omega)$ is in the same units. The text discusses the significance of the arrows in panels (a) and (c).

structures are very similar, suggesting that the slight difference in measured a and b lattice parameters plays a minor role in the magnetic structure. Experimental lattice parameters were employed.[12]

In Fig. 1(a), the density of states $N(E)$ is shown over a 2-eV energy window for a small and large moment case ($M = 0.4\mu_B$ and $1.1\mu_B$). Particularly of note is a sharp peak near E_F, of width ~ 50 meV. This narrow band is found to consist almost entirely of majority-spin Fe d_{xy} and d_{yz} orbitals. The peak falls slightly below E_F for $M = 0.4\mu_B$ and slightly above for $M = 1.1\mu_B$. Thus, as R_{Fe-As} is smoothly varied so that M changes continuously, this peak passes through E_F. As a result, $N(E_F)$ reaches a maximum around $M = 0.8\mu_B$ [Fig. 1(b)]. The fact that this unusual dependence originates in the magnetic part of the Hamiltonian can be verified by repeating the calculation in the nonmagnetic case. As Fig. 1(b) shows, the nonmagnetic $N(E_F)$ is large, and approximately independent of R_{Fe-As}. In summary, the magnetic splitting produces a pseudogap in $N(E)$ for large M; the pseudogap shrinks as M decreases and causes a narrow band of Fe d states to pass through E_F, creating a sharp maximum in $N(E_F)$ near $M = 0.8\mu_B$. As we will show in the following, this moment demarcates a point of transition from itinerant to localized behavior (see also Ref. 13).

Next we turn to magnetic excitations. In the standard picture of magnons, Im$\chi_0(\omega)$ is significant only for frequencies exceeding the magnetic (Stoner) splitting of the d bands, $\epsilon_d^{\downarrow} - \epsilon_d^{\uparrow} = IM$ [cf. Eq. (2)]. In such cases, Imχ_0 is small at low (q, ω) and well-defined magnons appear at energies near $|1 - I\text{Re}\chi_0| = 0$ [cf Eq. (1)]. As Imχ_0 increases, the SW spectrum $\bar{\omega}(\mathbf{q})$ broadens; as Imχ_0 becomes large, the spectrum can become incoherent, or (Stoner) peaks can arise from Imχ_0, possibly enhanced by small $1 - I\text{Re}\chi_0$. Figure 1(c) shows Im$\chi_0(q = 0, \omega)$ on a broad energy scale. The description of $N(E)$ leads to a classification of Stoner transitions into three main types.

(1) Excitations from the usual Stoner splitting: In a rigid-band model, no bands are spin split but the d states, which are split by IM. Only they contribute to Im$\chi_0(q = 0, \omega)$ because all other pairs of states are spatially orthogonal and their cell average vanishes. The vertical arrows in Fig. 1(c) demarcate IM, assuming $I \approx 1$ eV known to apply to $3d$ transition metals. Peaks that approximately correspond to IM we identify with the usual Stoner splitting. The splitting can be

seen in the density of states (DOS), Fig. 1(a), for $M = 1.1\mu_B$; it is indicated by a large red arrow showing transitions between Fe states (largely, d_{xz} and d_{xy}) near -0.4 eV to unoccupied d states below 1 eV.

(2) Transitions to states of (d_{xy}, d_{yz}, d_{xz}) character just above the psuedogap, depicted by a small arrow near 1.2 eV in Fig. 1(a), and slanting arrows in Fig. 1(d): These are the excitations probably detected in neutron measurements.[4,5] This pseudogap is well defined for $M \gtrsim 1.1\mu_B$, but is modified as M decreases, which leads to the following.

(3) Near $M = 0.8\mu_B$, the narrow d band passes through E_F, opening up channels, not previously considered, for low-energy, particle-hole transitions within this band. When M reaches $0.4\mu_B$, this band has mostly passed through E_F and the pseudogap practically disappears.

What makes the pnictide systems so unusual is that Imχ_0 is already large at very low energies (~ 10 meV) once the sharp peak in $N(E)$ approaches E_F. One of our central findings is that this system undergoes a transition from localized to a coexistence of localized and itinerant behavior as M decreases from $M \gtrsim 1.1\mu_B$ to $M \approx 0.8\mu_B$. Moreover, the itinerant character is of an unusual type: elementary excitations are mostly single-particle-hole like and they can be well defined in energy and q. These represent *coherent* excitations. The dependence of $N(E_F)$ on M is not only responsible for them, but also may explain the unusual linear temperature dependence of paramagnetic susceptibility, and the appearance of a Lifshitz transition with Co doping.[14]

Figure 2 focuses on the antiferromagnetic (AFM) line $\mathbf{q} = [H00]2\pi/a$. Panel (a) shows the full Im$\chi(\omega)$ for $M = 1.1\mu_B$ for several q points spanning the entire line $0 < H < 1$. At low q, peaks $\bar{\omega}$ in χ are sharp, and $\bar{\omega}$ depends on H in the expected manner ($\bar{\omega} \propto H$). The $\bar{\omega}$ reaches a maximum near $H = 1/2$ [Fig. 2(b)] for all three values of M. The peaks broaden with increasing q; nevertheless, we can associate them with magnons because they coincide closely with vanishing $|1 - I\text{Re}\chi_0|$ and Γ is not too large. The magnon character is preserved for most q at all moments, as Fig. 2(b) shows; but, for $H > 0.8$, the peaks are strongly broadened, especially for small M. The $\bar{\omega}$ is in good agreement with neutron data of Ref. 5, except that neutron data are apparently smaller than the large M calculations predict.[15]
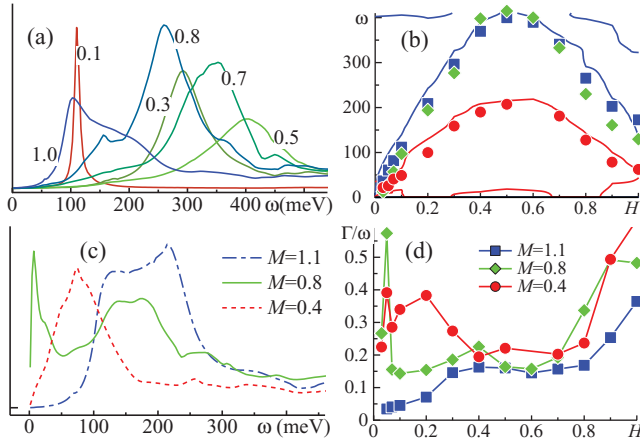
FIG. 2. (Color online) $\mathrm{Im}\chi(\mathbf{q},\omega)$ along the AFM axis $\mathbf{q} = [H,0,0]2\pi/a$. (a) $\mathrm{Im}\chi(\omega)$ for various H and $M = 1.1\mu_B$. Extracted from $\mathrm{Im}\chi(H,\omega)$ are peak positions $\bar\omega(H)$ (meV) and half-width at half-maximum Γ. (b) and (d) depict $\bar\omega$ and the ratio $\Gamma/\bar\omega$, for the three moments shown in the key. Panel (b) also depicts, as solid lines, contours $|1 - I\mathrm{Re}\chi_0| = 0$ in the (ω,H) plane, for $M = 1.1\mu_B$ and $0.4\mu_B$. Panel (c) shows $\mathrm{Im}\chi(H = 0.9,\omega)$ for the three moments.

One experimental measure of the validity of the local-moment picture is the ratio of half-width at half-maximum Γ to $\bar\omega$, shown in Fig. 2(d). For large M and most of q, $\Gamma/\bar\omega \sim 0.15$–0.18. For intermediate and small M, $\Gamma/\bar\omega \geqslant 0.2$ for a wide diapason of q. This is significant: it reflects the increasing Stoner character of the elementary excitations. If there were an abrupt transition into a conventional Stoner continuum as argued in Ref. 5, it would be marked by an abrupt change in $\Gamma/\bar\omega$. This is not observed; yet, damping appears to increase with energy and q, reflecting normal metallic behavior.

Spectra for $H = 0.9$ [Fig. 2(c)] adumbrate two important findings of this work. When $M = 0.8\mu_B$, a sharp peak in $\chi(\omega)$ appears near 10 meV. There is a sharp peak in $\chi_0(\omega)$ at $\bar\omega \approx 10$ meV also, classifying this as a particle-hole excitation originating from the narrow d band depicted in Fig. 1. Being well defined in energy, it is coherent, analogous to a SW, only with a much larger $\Gamma/\bar\omega$. Yet, it is strongly enhanced by collective interactions, since $|1 - I\mathrm{Re}\chi_0|$ ranges between 0.1 and 0.2 for $\omega < 100$ meV. This new kind of itinerant excitation will be seen at many values of q, typically at small q. The reader many note the sharp rise and fall in $\Gamma/\bar\omega$ at small q in Fig. 2(d). This anomaly reflects a point where a SW and a particle-hole excitation coalesce to the same $\bar\omega$.

Returning to $H = 0.9$ when $M = 1.1$, there is a standard (broadened) SW at 200 meV [cf. contours in Fig. 2(b)]. A *second*, low-energy excitation can be resolved near 120 meV. There is no corresponding zero in the denominator in Eq. (1), but no strong peak in $\chi_0(\omega)$ either. This excitation must be classified as a hybrid intermediate between Stoner excitations and SWs. Only a single peak remains when $M = 0.4\mu_B$ and the peak in $N(E)$ has mostly passed through E_F (Fig. 1).

Along the ferromagnetic (FM) line $\mathbf{q} = (0,K,0)2\pi/a$, $\chi(\omega)$ is more complex and more difficult to interpret. At $M = 1.1\mu_B$ sharp, well-defined collective excitations are found at low q, and broaden with increasing q. There is a reasonably close
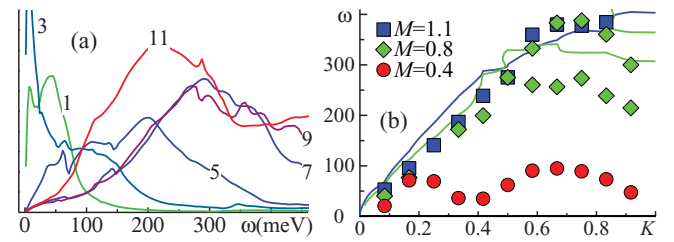

FIG. 3. (Color online) $\mathrm{Im}\chi(\mathbf{q},\omega)$ along the FM axis, $\mathbf{q} = [0,K,0]2\pi/a$. (a) $\mathrm{Im}\chi(\omega)$ at $K = 1/12, 3/12, 5/12, 7/12, 9/12$, and $11/12$ for $M = 0.8\mu_B$. Strong Stoner excitations can be seen for $K = 1/12$ and $3/12$ near $\bar\omega \sim 10$–20 meV. (b) Contours $|1 - I\mathrm{Re}\chi_0| = 0$ in the (ω,K) plane for $M = 1.1\mu_B$ and $0.8\mu_B$, analogous to Fig. 2(b), and dominant peak positions $\bar\omega$ obtained by a nonlinear least-squares fit of one or two Gaussian functions to $\chi(\omega)$ over the region where peaks occur.

correspondence with the zeros of $|1 - I\mathrm{Re}\chi_0|$ and peaks in χ, as Fig. 3(b) shows. The $M = 0.8\mu_B$ case is roughly similar, except that, for $K > 0.4$, excitations can not be described by a single peak. Note that, for fixed q, propagating spin fluctuations (characterized by peaks at $\bar\omega$) can exist at *multiple energies,* with the magnetic analog of the dielectric function passing through zero and sustaining plasmons at multiple energies. Peaks in $\chi(\omega)$ can broaden as a consequence of this; the $K = 7/12, 9/12$, and $11/12$ data of Fig. 3(a) are broadened in part by this mechanism as distinct from the usual one (intermixing of Stoner excitations). Second, consider how $\partial\bar\omega/\partial q$ changes with M for $K > 0.5$ [Fig. 3(b)]. When $M = 1.1\mu_B$, $\bar\omega$ increases monotonically with K. For $M = 0.8\mu_B$, $\bar\omega$ has a complex structure, but apparently reaches a maximum before K reaches 1. The fact that $\partial\bar\omega/\partial q$ changes sign is significant: it marks the disappearance of magnetic frustration between the ferromagnetically aligned spins at low moments and the emergence of stable FM order along [010], characteristic of local-moment behavior (see also Ref. 16). Experimentally, Ref. 5 reports $\partial\bar\omega/\partial q > 0$ for $K > 0.5$. While our calculations provide a clear physical interpretation, we note significant differences in the moment where we observe this effect ($M = 0.8$–$1.1\mu_B$) and the effective spin ($S = 0.2$) used in Ref. 5. Finally, we find that the collective mode frequencies (spin-wave spectrum) only weakly depend on M, even for large M.

Elementary excitations along the c axis $\mathbf{q} = (0,0,L)2\pi/c$ bring into highest relief the transition from pure local-moment behavior (collective excitations) to one where coherent itinerant Stoner and collective excitations coexist. Collective excitations are found for all L and all M. For $M = 1.1\mu_B$, a single peak is found; excitations are well described by the Heisenberg model with weak damping. Comparing Fig. 4(b) to Figs. 2(b) and 3(b), it is apparent that $\bar\omega$ rises much more slowly along L than along H or K, confirming that interplane interactions are weak. When M drops to $0.8\mu_B$, a second low-energy peak at $\bar\omega'$ emerges at energies below 20 meV for small q along $[0,K,0]$ and for all q along $[0,0,L]$, coexisting with the collective excitation. Why these transitions are absent for $M = 1.1\mu_B$ and are so strong at $M = 0.8\mu_B$ can be understood in terms of roughly cylindrical Fermi surface at
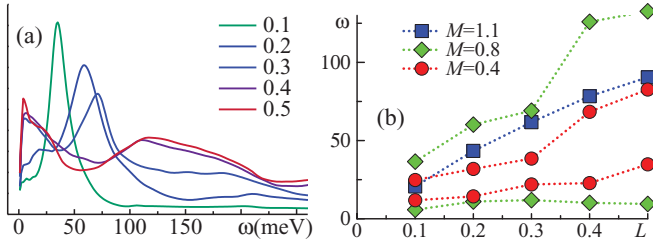
FIG. 4. (Color online) $\mathrm{Im}\chi(\mathbf{q},\omega)$ along the c axis, $\mathbf{q} = [0,0,L]2\pi/c$. (a) $\mathrm{Im}\chi(\omega)$ at values of L listed in the key, for $M = 0.8\mu_B$. When $M = 1.1\mu_B$ (not shown), the spectrum is well characterized by a single sharp peak at any L. When $M = 0.8$ or $0.4\mu_B$, the SW peak remains, but a low-energy Stoner excitation coexists with it. The latter are most pronounced for larger L, but can be resolved at every L. (b) The peak positions are shown (single for $M = 1.1\mu_B$, double for $M = 0.8$ and $0.4\mu_B$).

$k = (1/2,0,k_z)$. Single spin-flip transitions between occupied states $\epsilon_{\mathbf{k}}^{\uparrow}$ and unoccupied states $\epsilon_{\mathbf{k}+\mathbf{q}}^{\downarrow}$ separated by ~ 10 meV are responsible for this peak [see Eq. (2)]. They originate from "hot spots" where $N(\epsilon_{\mathbf{k}}^{\uparrow})$ and $N(\epsilon_{\mathbf{k}+\mathbf{q}}^{\downarrow})$ are both large.

From the SW velocities $(\partial\bar{\omega}/\partial q)_{q=0}$, anisotropy of the exchange couplings can be determined.[7,16,17] We find moderate in-plane and out-of-plane anisotropies, and predict $v_b/v_a = 0.55$ and find $v_c/v_a = 0.35$, where $v_a = 490$ meV· Å. Neutron scattering experiments[3,17] have measured v_c/v_{a-b} to be ~ 0.2–0.5.

In summary, we broadly confirm the experimental findings of Refs. 4 and 5 that there is a spectrum of magnetic excitations of the striped phase of $CaFe_2As_2$, which, for the most part, are weakly damped at small q and more strongly damped at large q. A new kind of excitation was found, which originates from single-particle-hole transitions within a narrow band of states near E_F, renormalized by a small denominator $|1 - I\mathrm{Re}\chi_0|$. They appear when the Fe moment falls below a threshold, at which point the narrow band passes through E_F. The character of itineracy is novel: excitations occur at low energy, at energy scales typically below T_N, and can be sharply peaked, and thus coherent. The distinction between the two kinds of excitations is particularly observable in the anomalous dependence of $\Gamma/\bar{\omega}$ on q in Fig. 2(d). Collective spin-wave-like excitations also are unusual; multiple branches are found at some q. Finally, at higher q, we find that the SW velocity changes sign, which is also observed experimentally at similar values of M.

Overall, a picture emerges where localized and itinerant magnetic carriers coexist and influence each other. This description falls well outside the framework of a local-moments model such as the Heisenberg Hamiltonian. Additional low-energy neutron experiments are required to check the existence of these itinerant excitations.

[1] I. I. Mazin, Nature (London) **464**, 183 (2010).

[2] D. C. Johnston, Adv. Phys. **59**, 803 (2010).

[3] J. W. Lynn and P. Dai, Phys. C (Amsterdam) **469**, 469 (2009).

[4] S. O. Diallo, V. P. Antropov, T. G. Perring, C. Broholm, J. J. Pulikkotil, N. Ni, S. L. Bud'ko, P. C. Canfield, A. Kreyssig, A. I. Goldman, and R. J. McQueeney, Phys. Rev. Lett. **102**, 187206 (2009).

[5] J. Zhao, D. T. Adroja, D. Yao, R. Bewley, S. Li, X. Wang, G. Wu, X. Chen, J. Hu, and P. Dai, Nat. Phys. **5**, 555 (2009).

[6] M. D. Johannes and I. I. Mazin, Phys. Rev. B **79**, 220510 (2009); I. I. Mazin and J. Schmalian, Phys. C (Amsterdam) **469**, 614 (2009).

[7] Z. P. Yin, S. Lebègue, M. J. Han, B. P. Neal, S. Y. Savrasov, and W. E. Pickett, Phys. Rev. Lett. **101**, 047001 (2008).

[8] C. Fang, H. Yao, W. F. Tsai, J. P. Hu, and S. A. Kivelson, Phys. Rev. B **77**, 224509 (2008); F. Kruger, S. Kumar, J. Zaanen, and J. van den Brink, *ibid.* **79**, 054504 (2009); C. C. Lee, W. G. Yin, and W. Ku, Phys. Rev. Lett. **103**, 267001 (2009).

[9] T. Kotani, M. van Schilfgaarde, and S. V. Faleev, Phys. Rev. B **76**, 165106 (2007).

[10] T. Kotani and M. van Schilfgaarde, J. Phys. Condens. Matter **20**, 295214 (2008).

[11] R. Martin, *Electronic Structure* (Cambridge University Press, Cambridge, 2004).

[12] A. I. Goldman, D. N. Argyriou, B. Ouladdiaf, T. Chatterji, A. Kreyssig, S. Nandi, N. Ni, S. L. Bud'ko, P. C. Canfield, and R. J. McQueene, Phys. Rev. B **78**, 100506 (2008).

[13] G. D. Samolyuk and V. P. Antropov, Phys. Rev. B **79**, 052505 (2009).

[14] N. Ni, A. N. Thaler, A. Kracher, J. Q. Yan, S. L. Bud'ko, and P. C. Canfield, Phys. Rev. B **80**, 024511 (2009); E. D. Mun, S. L. Bud'ko, N. Ni, A. N. Thaler, and P. C. Canfield, *ibid.* **80**, 054517 (2009).

[15] The origin of the discrepancy in $\bar{\omega}$ with experiment is not clear. It could be related to the LSDA overestimate of magnetic moment in ferropnictides.

[16] J. J. Pulikkotil1, L. Ke, M. van Schilfgaarde, T. Kotani, and V. P. Antropov, Supercond. Sci. Technol. **23**, 054012 (2010).

[17] R. J. McQueeney, S. O. Diallo, V. P. Antropov, G. D. Samolyuk, C. Broholm, N. Ni, S. Nandi, M. Yethiraj, J. L. Zarestky, J. J. Pulikkotil, A. Kreyssig, M. D. Lumsden, B. N. Harmon, P. C. Canfield, and A. I. Goldman, Phys. Rev. Lett. **101**, 227205 (2008).